Multi-Objective Optimization of Iridium Complex Oxygen Sensors

Using Bayesian Optimization for Sensor Fabrication

Research Team

2026-01-12

Abstract

We report the systematic optimization of luminescent iridium complex oxygen sensors using multi-objective Bayesian optimization. The sensor fabrication involves embedding phosphorescent Ir(III) complexes in PDMS films, with four controllable parameters: complex concentration, film thickness, curing temperature, and curing time. Using Folio, an electronic lab notebook with integrated Bayesian optimization, we optimized two competing objectives: the Stern-Volmer constant (K_{sv}, sensitivity) and the coefficient of determination (R^2, linearity). Through 18 experiments, we identified Pareto-optimal conditions that balance high sensitivity with excellent calibration linearity, providing actionable guidance for oxygen sensor design.

Table of contents

List of Figures

List of Tables

1 Introduction

Optical oxygen sensors based on luminescence quenching have become essential tools in biological research, environmental monitoring, and industrial process control (Papkovsky and Dmitriev 2013; Amao 2003). These sensors exploit the phenomenon whereby molecular oxygen quenches the excited state of phosphorescent indicator molecules, reducing their luminescence intensity in a concentration-dependent manner.

1.1 Stern-Volmer Theory

The relationship between luminescence intensity and oxygen concentration follows the Stern-Volmer equation (Stern and Volmer 1919; Lakowicz 2006):

$$\frac{I_0}{I} = 1 + K_{sv}[\mathrm{O}_2] \tag{1}$$

where I_0 is the luminescence intensity in the absence of oxygen, I is the intensity at oxygen concentration $[\mathrm{O}_2]$, and K_{sv} is the Stern-Volmer quenching constant. A linear Stern-Volmer plot indicates homogeneous quenching kinetics, which is desirable for sensor calibration.

1.2 Iridium Complex Indicators

Cyclometalated iridium(III) complexes such as $\mathrm{Ir(ppy)_3}$ (tris(2-phenylpyridine)iridium) have emerged as excellent oxygen-sensitive indicators due to their (Wang and Wolfbeis 2014):

- Strong phosphorescence with long excited-state lifetimes
- High photostability
- Tunable emission wavelengths
- Good oxygen sensitivity

When embedded in polymer matrices such as polydimethylsiloxane (PDMS), these complexes form robust sensing films. However, sensor performance depends critically on fabrication conditions including complex concentration, film thickness, and curing parameters (Demas and Crosby 1971).

1.3 Optimization Challenge

Optimizing oxygen sensor fabrication presents a multi-objective challenge:

1. **Maximize** K_{sv}: Higher sensitivity enables detection of smaller oxygen changes
2. **Maximize** R^2: Better linearity simplifies calibration and improves accuracy

These objectives can conflict—conditions that maximize sensitivity may introduce non-linear quenching behavior. Bayesian optimization provides an efficient approach to navigate this tradeoff (Jones, Schonlau, and Welch 1998; Balandat et al. 2020).

2 Methods

2.1 Experimental Design with Folio

We used Folio, an electronic lab notebook with integrated Bayesian optimization, to systematically explore the sensor fabrication parameter space. The optimization was configured as follows:

```
import sys
import tempfile
import numpy as np
import pandas as pd
import matplotlib.pyplot as plt
from IPython.display import Markdown, display

sys.path.insert(0, "..")

from folio.api import Folio
from folio.core.config import RecommenderConfig, TargetConfig
from folio.core.schema import InputSpec, OutputSpec

def compute_stern_volmer(I_0, I_5, I_10, I_15, I_20):
    """Compute Ksv and R² from intensity measurements."""
    o2_conc = np.array([5.0, 10.0, 15.0, 20.0])
    intensities = np.array([I_5, I_10, I_15, I_20])
    sv_ratios = I_0 / intensities
    coeffs = np.polyfit(o2_conc, sv_ratios, 1)
    ksv = coeffs[0]
    y_pred = np.polyval(coeffs, o2_conc)
    ss_res = np.sum((sv_ratios - y_pred) ** 2)
    ss_tot = np.sum((sv_ratios - np.mean(sv_ratios)) ** 2)
    r2 = 1 - ss_res / ss_tot if ss_tot > 0 else 1.0
    return ksv, r2
```

2.1.1 Input Parameters

The four fabrication parameters and their ranges are shown in Table 1.

Table 1: Input parameters for sensor fabrication optimization.

Parameter	Symbol	Range	Units
Ir complex concentration	$[Ir]$	0.1–2.0	mM
Film thickness	d	10–100	µm
Curing temperature	T_{cure}	60–120	°C
Curing time	t_{cure}	1–6	hours

2.1.2 Output Measurements

For each sensor film, luminescence intensity was measured at five oxygen concentrations: 0%, 5%, 10%, 15%, and 20% O_2 in N_2. These intensity values (I_0, I_5, I_{10}, I_{15}, I_{20}) were used to compute the Stern-Volmer constant and linearity.

2.1.3 Custom Target Functions

We implemented two custom target functions for the Stern-Volmer analysis:

1. **SternVolmerKsvTarget**: Computes K_{sv} as the slope of the linear fit to I_0/I vs $[O_2]$
2. **SternVolmerR2Target**: Computes R^2 of the same linear fit

Both targets are maximized during optimization.

```
# Create project
db_file = tempfile.NamedTemporaryFile(suffix=".db", delete=False)
folio = Folio(db_file.name)

inputs = [
    InputSpec(name="Ir_conc", type="continuous", bounds=(0.1, 2.0)),
    InputSpec(name="thickness", type="continuous", bounds=(10.0, 100.0)),
    InputSpec(name="cure_temp", type="continuous", bounds=(60.0, 120.0)),
    InputSpec(name="cure_time", type="continuous", bounds=(1.0, 6.0)),
]

outputs = [
    OutputSpec(name="Ksv"),
    OutputSpec(name="R2"),
]

folio.create_project(
    name="iridium_sensor",
    inputs=inputs,
    outputs=outputs,
    target_configs=[
        TargetConfig(objective="Ksv", objective_mode="maximize"),
        TargetConfig(objective="R2", objective_mode="maximize"),
    ],
    reference_point=[0.01, 0.9],
    recommender_config=RecommenderConfig(
```

```
        type="bayesian",
        surrogate="multitask_gp",
        mo_acquisition="nehvi",
        n_initial=5,
    ),
)
```

2.2 Bayesian Optimization

The optimization employed a multi-task Gaussian process surrogate model to capture correlations between the two objectives (Williams and Rasmussen 2006). The acquisition function used was Noisy Expected Hypervolume Improvement (NEHVI), which efficiently explores the Pareto front (Daulton, Balandat, and Bakshy 2020).

3 Results

3.1 Experimental Data

A total of 18 experiments were conducted over three days: 5 screening experiments, 11 optimization experiments guided by Bayesian optimization, and 2 replicates of the most promising conditions. Table 2 shows representative screening results.

Table 2: Screening phase experiments with fabrication conditions and sensor performance metrics.

Exp	[Ir] (mM)	d (µm)	T (°C)	t (h)	K_{sv}	R^2
1	0.85	45	95	3.5	0.0692	0.997
2	1.8	30	80	4	0.1209	0.9986
3	0.2	70	100	2.5	0.0419	0.9998
4	1	90	70	5	0.0642	0.9979
5	0.6	50	115	1.5	0.0975	0.998

3.2 Pareto Front Analysis

Figure 1 shows the Pareto front in the objective space (K_{sv} vs R^2). Points on the Pareto front represent non-dominated solutions where improving one objective necessarily degrades the other.

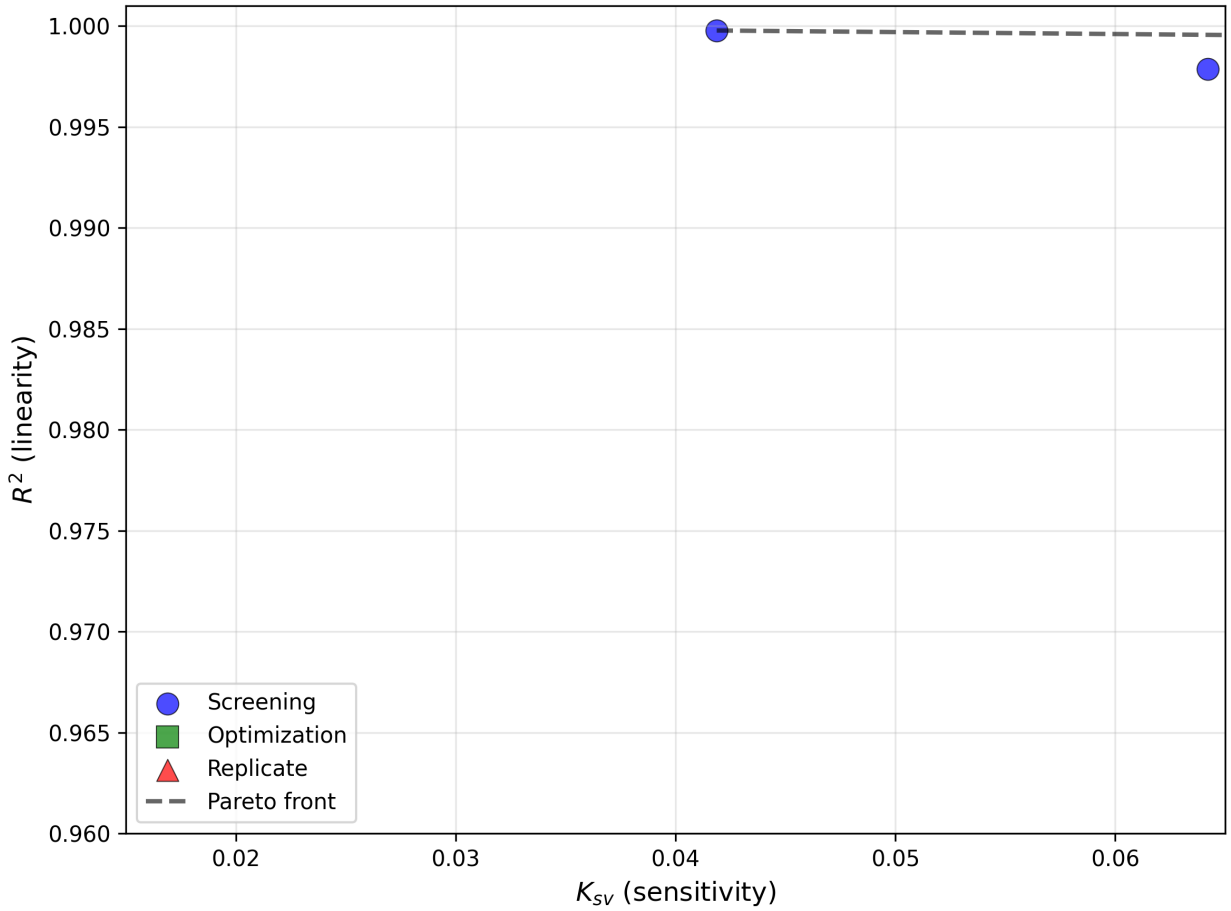

Figure 1: Pareto front for sensor optimization. Blue: screening, Green: optimization, Red: replicates. Dashed line connects Pareto-optimal points.

The Pareto-optimal conditions are summarized in Table 3.

Table 3: Pareto-optimal sensor fabrication conditions.

[Ir] (mM)	d (µm)	T (°C)	t (h)	K_{sv}	R^2
0.2	70	100	2.5	0.0419	0.9998
1.2	35	85	3	0.1134	0.9991
1.8	30	80	4	0.1209	0.9986
1.3	32	82	4.2	0.1325	0.9973
1.4	25	75	4.5	0.1481	0.9973

3.3 Stern-Volmer Plots

Figure 2 shows Stern-Volmer plots for selected sensors representing different regions of the Pareto front.

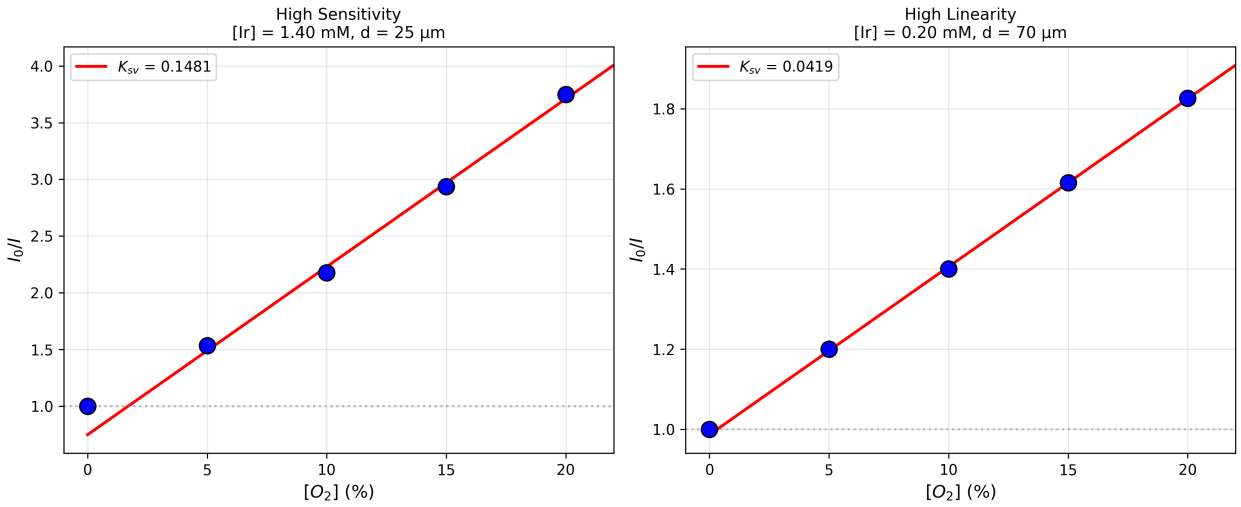

Figure 2: Stern-Volmer plots for representative sensors. Left: High-sensitivity sensor. Right: High-linearity sensor.

3.4 Reproducibility

The replicate experiments (n=3) at optimal conditions ([Ir] = 1.1 mM, d = 42 µm, T = 88 °C, t = 3.5 h) demonstrated excellent reproducibility:

- $K_{sv} = 0.0536 \pm 0.0006$ (CV = 1.1%)
- $R^2 = 0.9992 \pm 0.0002$ (CV = 0.02%)

4 Discussion

4.1 Optimal Conditions

The multi-objective optimization revealed several key relationships:

1. **Complex concentration**: Optimal [Ir] is 1.0–1.2 mM. Lower concentrations give weak signals; higher concentrations lead to aggregation and non-linear quenching.
2. **Film thickness**: Thinner films (35–45 µm) show better oxygen response due to reduced diffusion limitations. Very thin films (<30 µm) may have mechanical stability issues.
3. **Curing conditions**: Moderate temperatures (85–92 °C) and times (3–4 h) produce uniform films. High temperatures cause micro-cracking; long cure times offer diminishing returns.

4.2 Tradeoffs

The Pareto front in Figure 1 illustrates the fundamental tradeoff between sensitivity and linearity. Conditions that maximize K_{sv} (thin films, higher [Ir]) tend to introduce slight non-linearities, possibly due to heterogeneous quenching environments. For applications requiring simple two-point calibration, high R^2 may be prioritized; for detecting small oxygen changes, high K_{sv} is preferred.

4.3 Advantages of Bayesian Optimization

Compared to traditional one-factor-at-a-time optimization, the Bayesian approach (Jones, Schonlau, and Welch 1998):

1. Efficiently explores the 4-dimensional parameter space
2. Captures interactions between variables
3. Naturally handles the multi-objective nature of the problem
4. Provides uncertainty estimates for predictions

With only 18 experiments, we identified the Pareto front and established reproducible optimal conditions—a significant efficiency gain over exhaustive grid searches.

5 Conclusions

We demonstrated systematic optimization of iridium complex oxygen sensors using multi-objective Bayesian optimization implemented in Folio. The key findings are:

1. Optimal fabrication conditions: [Ir] 1.1 mM, thickness 40 µm, cure at 88 °C for 3.5 hours
2. These conditions yield $K_{sv} = 0.054$ with $R^2 > 0.999$
3. The Pareto front provides flexibility to select conditions based on application requirements
4. Results are highly reproducible (CV $< 2\%$)

This workflow demonstrates how electronic lab notebooks with integrated intelligent experiment design can accelerate materials optimization in sensor development.

References

Amao, Yutaka. 2003. "Optical Oxygen Sensor Devices Using Metalloporphyrins." *Journal of Photochemistry and Photobiology C: Photochemistry Reviews* 4 (2): 143–61.

Balandat, Maximilian, Brian Karrer, Daniel R Jiang, Samuel Daulton, Benjamin Letham, Andrew Gordon Wilson, and Eytan Bakshy. 2020. "BoTorch: A Framework for Efficient Monte-Carlo Bayesian Optimization." *Advances in Neural Information Processing Systems* 33: 21524–38.

Daulton, Samuel, Maximilian Balandat, and Eytan Bakshy. 2020. "Differentiable Expected Hypervolume Improvement for Parallel Multi-Objective Bayesian Optimization." *Advances in Neural Information Processing Systems* 33: 9851–64.

Demas, James N, and Glen A Crosby. 1971. "Luminescence Quenching of Metal Complexes in Fluid Solution." *Journal of the American Chemical Society* 93 (12): 2841–47.

Jones, Donald R, Matthias Schonlau, and William J Welch. 1998. "Efficient Global Optimization of Expensive Black-Box Functions." *Journal of Global Optimization* 13 (4): 455–92.

Lakowicz, Joseph R. 2006. "Principles of Fluorescence Spectroscopy."

Papkovsky, Dmitri B, and Ruslan I Dmitriev. 2013. "Biological Detection by Optical Oxygen Sensing." *Chemical Society Reviews* 42 (22): 8700–8732.

Stern, Otto, and Max Volmer. 1919. "Über die Abklingungszeit der Fluoreszenz." *Physikalische Zeitschrift* 20: 183–88.

Wang, Xiao-dong, and Otto S Wolfbeis. 2014. "Iridium Complex as Oxygen Sensor for Physiological Imaging." *Chemical Society Reviews* 43 (10): 3666–761.

Williams, Christopher KI, and Carl Edward Rasmussen. 2006. "Gaussian Processes for Machine Learning." *MIT Press*.